Chain-Length-Dependent Correlated Molecular Motion in Polymers

Matthew Reynolds,[1] Daniel L. Baker,[1] Peter D. Olmsted,[2] and Johan Mattsson[1,*]
[1]School of Physics and Astronomy, University of Leeds, Leeds LS2 9JT, United Kingdom
[2]Department of Physics and Institute for Soft Matter Synthesis and Metrology, Georgetown University, Washington, DC 20057, USA

(Received 4 May 2024; revised 10 June 2025; accepted 27 October 2025; published 17 November 2025)

We show how dynamic heterogeneities (DHs), a hallmark of glass-forming materials, depend on chain flexibility and chain length in polymers. For highly flexible polymers, a relatively large number of monomers ($N_c \sim 500$) undergo correlated motion at the glass transition temperature (T_g), independent of molecular weight (M). In contrast, less flexible polymers show a complex $N_c(M)$ behavior divided into three regimes, consistent with observations in both $T_g(M)$ and chain conformational structure. For short oligomers ($\lesssim$2 Kuhn steps), a transition from mainly intermolecular correlations and $N_c \sim 200$ to strongly intramolecular correlations and $N_c < 50$ (roughly the molecular size) is observed; for longer chains, N_c increases weakly, before saturating. For poly(methyl methacrylate), a remarkable similarity is found between $N_c(M)$ and the M-dependent ratio of the activation barriers of the structural (α) and secondary (β) relaxations; we present evidence that this relationship is a general feature of glass-forming polymers. Our results suggest a direct link between the DH length scale and the number of β relaxation events jointly activated to facilitate the α relaxation.

DOI: 10.1103/p5r4-2g4q

Introduction—Molecular motions in polymer melts slow down during cooling, eventually resulting in the formation of a disordered solid—a glass. The glass transition temperature T_g is defined as $\tau_\alpha(T_g) \equiv 100$ s [1], where $\tau_\alpha(T)$ is the temperature-dependent structural (α) relaxation time [2]. Near T_g, so-called dynamic heterogeneities (DHs), in which the local dynamics vary from place to place, become more prominent [3,4]. Their characteristic length scale ξ_{DH} has been determined for both polymeric and nonpolymeric liquids [5–9], using either experimental [9–16] or computational [17–23] approaches, with a resulting length scale $\xi_{\mathrm{DH}}(T_g) \sim 1$–5 nm [24], which for polymers correspond to $50-500$ monomers [7,9,25]. However, very few studies have investigated how polymer chain length affects DH [9,26,27] and the entire range from short oligomers to long-chain polymers has rarely been explored [27].

The glass transition of polymers and its associated dynamics can typically be divided into three distinct regimes [28,29], corresponding to (I) short oligomers ($\lesssim$2 Kuhn steps), (II) chains with $\sim 2-20$ Kuhn steps, and (III) long chains. These regimes are captured in the $T_g(M)$ behavior (segmental dynamics) and in the chain structure [29]. The inset to Fig. 1 shows an example for PMMA, illustrating $T_g(M)$ (open black symbols) and the M-dependent single-molecule aspect ratio $\Lambda^2(M) = \lambda_3(M)^2/\lambda_1(M)^2$ (solid green symbols), where λ_3^2 and λ_1^2 are the largest and smallest eigenvalues, respectively, of the average conformational tensor [29]. The regime I-II boundary at $M^\star$ is clearly manifested as both a kink in $T_g(M)$ and a peak in Λ^2, where the latter is due to chain folding occurring for $M \gtrsim M^\star$ [29]. For long chains in regime III ($> M^{\star\star}$), Λ^2 approaches the Gaussian chain value of $\approx$12.

To determine how chain length (or molecular weight M) affects DHs in polymers, we study four different polymer chemistries: poly(methyl methacrylate) (PMMA); polystyrene (PS); poly(propylene glycol dimethyl ether) (PPG-DME), and poly(dimethyl siloxane) (PDMS). PMMA and PS show relatively high T_g, dynamic fragility m [the sensitivity of $\tau_\alpha(T)$ to a T variation near T_g], and chain stiffness [30], whereas PPG-DME and PDMS are significantly more flexible polymers characterized by lower T_g and m.

DHs can be characterized by a "four-point" correlation function $G_4(\boldsymbol{r}, t)$ that correlates the relaxation dynamics (probed by two-point correlators) in space and time. A space integration of $G_4(\boldsymbol{r}, t)$ yields a dynamic susceptibility $\chi_4(t)$, which quantifies the fluctuations around the average dynamics [4,19,22,31,32]. $\chi_4(t)$ is typically a nonmonotonic function with a peak $\chi_4^{\max}$ near $t_{\max} \simeq \tau_\alpha(T)$, where $\chi_4^{\max}$ is proportional to the volume of correlated motions, or, correspondingly, the number of monomer units $N_c^{(4)}$ that undergo correlated motions.

*Contact author: k.j.l.mattsson@leeds.ac.uk

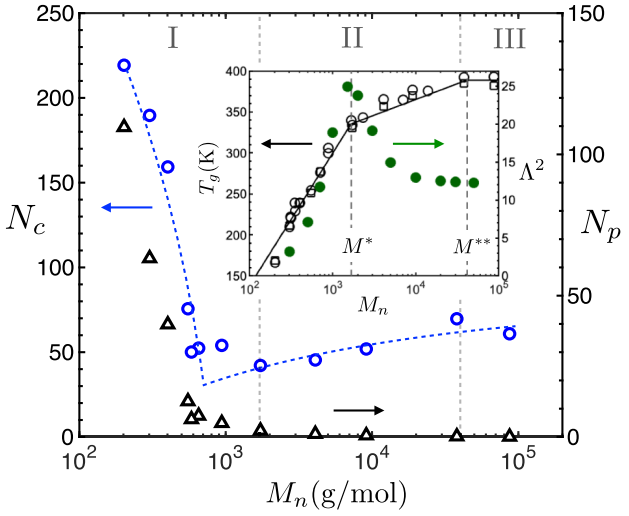

FIG. 1. (Left; blue circles) The number of monomers N_c involved in the α relaxation at $T_\alpha \simeq T_g$ for PMMA, determined using TMDSC. (Right; black triangles) $N_p \equiv N_c/n$, where n is the degree of polymerization. For short chains, where the behavior is intermolecular, N_p is roughly the number of molecules involved in the α relaxation. In contrast, $N_p \sim 1$ for $M \sim M^*$, which demonstrates the importance of intramolecular dynamics for $M \geq M^*$. The dashed (blue) lines are guides to the eye. The dotted vertical lines mark the regime boundaries at M^* and M^{**}, as shown in the inset. Inset: the M dependence of T_g (left) and the average polymer aspect ratio Λ^2 (right), from Baker *et al.* [29]. The dotted vertical lines in the main panel and the inset mark the regime boundaries at M^* and M^{**}.

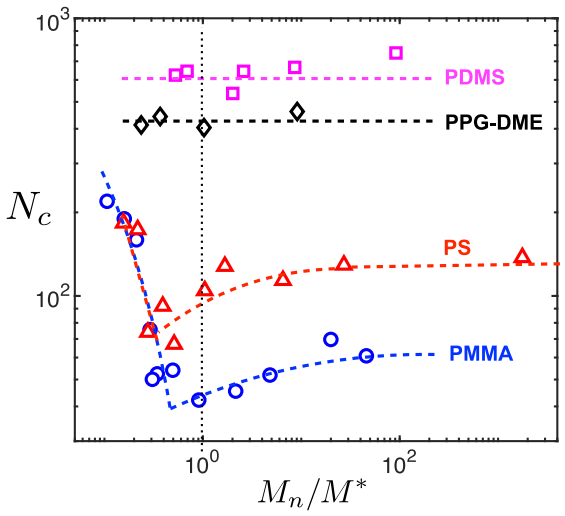

FIG. 2. Comparison of the number of correlated monomers N_c involved in the α relaxation for four different polymers as a function of molecular weight M_n, scaled by the molecular weight M^* separating regimes I and II.

Direct determination of $\chi_4(t)$ is difficult and has mainly been achieved in simulations [4,19,22] and for colloidal systems [33,34], as well as recently for a metallic glass former [35]. However, it has been demonstrated that $\chi_4(t)$ can be estimated from the temperature dependence of a dynamic susceptibility [31,32], obtained from broadband dielectric spectroscopy (BDS), rheology, or scattering [31,32].

We employ two approaches to determine the number of dynamically correlated units involved in the α relaxation [often referred to as a cooperatively rearranging region (CRR)]. The approach of Donth [11,36] yields the number of correlated units $N_c(T \sim T_g)$ from the thermal fluctuations measured near T_g using temperature modulated differential scanning calorimetry (TMDSC). The approach of Berthier *et al.* [31] estimates χ_4 from the temperature dependence of the complex permittivity measured using BDS, which then yields $N_c(T)$. We use both methods to determine the M dependence of N_c for the four investigated polymers and show in the End Matter that both approaches give consistent quantitative results.

Correlated dynamics—The results for $N_c(M)$ (at $T_\alpha \simeq T_g$; see End Matter for a detailed discussion) are shown for PMMA in blue rings in Fig. 1. We find that $N_c(M)$ falls dramatically in regime I from $N_c \sim 220$ for the dimer to $N_c < 50$ as the regime II boundary at $M^\star$ is approached. This demonstrates that near T_g the α relaxation dynamics for short oligomers (within regime I) are highly correlated, and since these molecules are very short, the dynamics are strongly intermolecular. This is further illustrated in black triangles in Fig. 1, which shows $N_p(M) = N_c(M)/n(M)$, where n is the degree of polymerization. For short chains $N_p(M)$ is roughly the M-dependent number of correlated molecules. We observe a drop from $N_p \sim 110$ for the dimer to $N_p \sim \mathcal{O}(1)$ near $M^\star$, reflecting strongly intramolecular behavior for $M \gtrsim M^\star$. Figure 1 shows that N_c increases slightly with M in regime II to reach $N_c \sim 60$ in regime III. Thus, the number of correlated monomers $N_c(M)$, as well as $T_g(M)$ and the chain structure $\Lambda^2(M)$ (inset of Fig. 1) all show distinct changes in behavior for similar characteristic molecular weights.

We compare $N_c(M)$ for all four polymers in Fig. 2. The stiffer polymers (PMMA and PS) show a sharp decrease of $N_c(M)$ in regime I, followed by a weak increase in regime II. However, the more flexible polymers (PPG-DME and PDMS) show a roughly constant $N_c(M)$, which exceeds that of the shortest PMMA and PS oligomers. For PPG-DME and PDMS, N_c is larger than the degree of polymerization n, i.e., $N_p > 1$, until regime III is reached.

These results suggest that intramolecular constraints are much weaker for PDMS and PPG-DME, so that chain connectivity and chain length do not significantly influence their α relaxation behavior, as demonstrated by the nearly M-independent $N_c \sim 300 - 700 \gg n$. Consistent with this, the rotational dihedral barriers of PPG-DME and PDMS (respectively, $\lesssim$1.0 [37] and 0.6 kcal/mole [38]) are

significantly smaller than those of PMMA and PS (respectively, 2.8 [39] and 3 kcal/mole [38]), and the O-Si-O bending energy for PDMS is notoriously weak [40].

For nonpolymeric glass formers and for short oligomers (in regime I), the molecular motions linked to the structural α relaxation are dominated by translational degrees of freedom (DOF). As chains with relatively high dihedral barriers (such as PMMA or PS) grow, the number of DOF available for molecular motions is reduced, by exchanging three intermolecular translational DOF for one dihedral intramolecular DOF (per additional degree of polymerization) [41]. This is accompanied by a change of the α relaxation character from mainly intermolecular to highly intramolecular. This is directly illustrated near the regime I-II crossover ($M \sim M^\star$), where chain folding takes place [29] and $N_c \sim n$. Correspondingly, as chains grow within regime I, less cooling is required for dynamic arrest to occur, meaning that fewer monomers are involved in correlated motions at T_g, as shown in Fig. 2.

Activation barriers—To further investigate the M dependence of N_c observed for PMMA and PS (Fig. 2), we first note that, in addition to the structural α relaxation, glass formers generally also show a faster β relaxation corresponding to more "local" cooperative motions [29]; there is significant evidence that the two relaxations are intrinsically linked [29,42].

Molecular relaxations in the glassy state typically follow the Arrhenius law, $\tau_i = \tau_{0i} \exp[\Delta H_i/RT]$ ($i = \alpha, \beta$), where $\tau_{0i} \sim 0.1$ ps is a microscopic relaxation time and R is the gas constant. Since $\tau_\alpha(T_g) \equiv 100$ s, $\Delta H_\alpha(M)|_{T=T_g} = RT_g \ln(100\ \mathrm{s}/\tau_0)$, while ΔH_β is T independent. Thus, $\Delta H_\alpha(M)|_{T=T_g}$ is proportional to $T_g(M)$, and both show three regimes in M [29] (inset to Fig. 1). While $\Delta H_\alpha(M)$ follows the M dependence of $T_g(M)$, $\Delta H_\beta(M)$ for PMMA increases with M in regime I and is nearly M independent in regimes II and III [29]. Hence, for PMMA the ratio $\mathcal{R}(M)$ obeys the M dependencies of both barriers in regime I, but mainly that of the α barrier in regimes II and III. Remarkably, as shown in Fig. 3, the ratio $\mathcal{R}(M) \equiv \Delta H_\alpha(M)/\Delta H_\beta(M)$ between the two activation barriers has an M dependence very similar to that of $N_c(M)$. Notably, $\mathcal{R}(M) \approx 1$ for $M \sim M^\star$, which corresponds to the onset of strongly intramolecular behavior in N_c (Fig. 1) and suggests a close correspondence between the properties of the α and the more local β relaxation (see a detailed discussion in [29]).

As discussed in Supplemental Material (Sec. E [43]), the similarities between the M dependence of $N_c(M)$ and the barrier ratio $\mathcal{R}(M)$ extend beyond PMMA. By combining our own data with the small amount of literature data, we find that $R(M)$ for PS and poly(α methyl styrene) behave similar to $R(M)$ for PMMA. Moreover, for the highly flexible polymers PDMS and PPG-DME, distinct β relaxations are not observed, but these polymers instead show

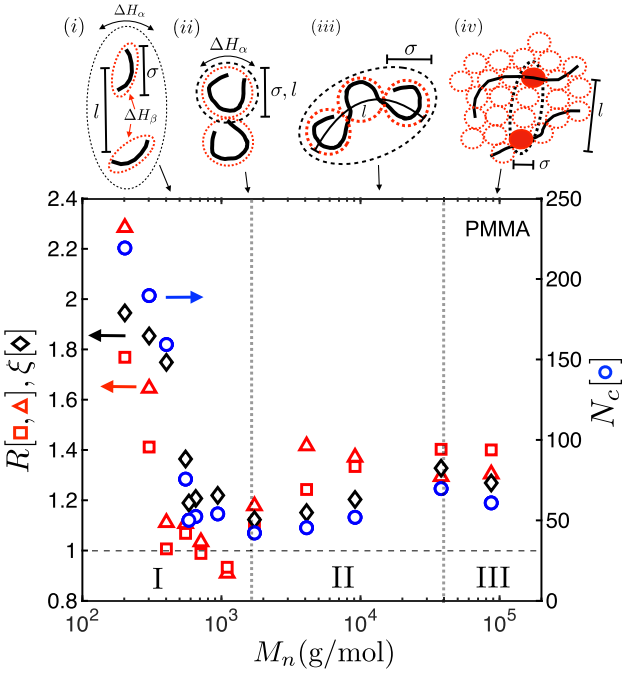

FIG. 3. Comparison between the molecular-weight-dependent ratio $\mathcal{R} = \Delta H_\alpha/\Delta H_\beta$ of α and β activation enthalpies of PMMA (left axis, red squares and triangles), characteristic length scale ξ_{DH} (black diamonds), and the number of correlated monomers N_c associated with the α relaxation (right axis, blue circles). Here, $\Delta H_\alpha(M) \equiv \Delta H_\alpha(M)|_{T=T_g}$ was estimated from $\tau_\alpha(T)$ using two different approaches (squares and triangles) following [29] and Supplemental Material [43]. The dotted vertical lines mark the regime boundaries at M^* and M^{**}. The cartoons (i)–(iv) illustrate the proposed relationship between the activation enthalpies for the α and β relaxations within the different regimes and are described in the text.

excess wings near T_g indicating highly "merged" β and α relaxations [68,69]. As discussed in Supplemental Material [43], we expect that such behavior should result in an effectively M-independent $\mathcal{R}(M)$, which is consistent with the M-independent behavior of $N_c(M)$ for PPG-DME and PDMS (Fig. 2). Hence, the observed correlation between $\mathcal{R}(M)$ and $N_c(M)$ appears to be general for polymers.

Both nonpolymeric and long-chain (regime III) polymeric glass formers often satisfy $\Delta H_\beta \approx 24RT_g$ [29,42,70], which suggests a typical value of the ratio, $\mathcal{R} \simeq \frac{1}{24}\ln(100\ \mathrm{s}/\tau_0) \approx 1.4$ and a direct link between the α and β relaxations. In fact, as long ago as 1940, Kauzmann and Eyring [71] suggested that flow in polymers results from "flow segments" comprising ~5–10 bonds. Numerous studies have since tried to link local dynamics, typically on the scale of the flow segment, to the structural α relaxation [72–77].

Dynamic facilitation—We recently suggested that the link between the α and β relaxations could be explained by "dynamic facilitation" (DF) [23,78,79], whereby a local

relaxation facilitates adjacent relaxations [23,29]. In polymers near T_g, we can apply DF to two situations: (1) For oligomers of stiffer polymers (such as PMMA or PS) at $T \sim T_g$, dense packing and relatively large dihedral barriers restrict local intramolecular motion to arise from cooperative motion, involving a few adjacent dihedral angles. These local cooperative rearrangements can propagate along the chain (intramolecular facilitation) and facilitate the rearrangement of the entire oligomer, resulting in the β relaxation and its associated enthalpy $\Delta H_\beta(M)$. (2) This newly mobile oligomeric chain can facilitate the mobility of other oligomers through intermolecular facilitation, to yield the α relaxation and its associated activation enthalpy $\Delta H_\alpha(T_g)$. For longer chains, chain folding divides the chain into β relaxation "beads," leading to a near constant $\Delta H_\beta(M^\star)$ for $M \geq M^\star$. Here, the structural α relaxation (and thus T_g) results from propagation of mobility through either intramolecular (along the chain) or intermolecular facilitation of the β beads; the nature of the facilitated dynamic coupling varies with chain length, thus separating $T_g(M)$ into distinct dynamic regimes (see schematic illustration in Fig. 3).

A hallmark of DF is hierarchical relaxations [78,79], where relaxation on one length scale facilitates adjacent relaxation on a larger length scale, leading to a logarithmic relationship between the length scale ℓ, separating fundamental excitations (relaxations) with energy ΔE_σ, and the activation barrier $\Delta E = \Delta E_\sigma[1 + \nu \log(\ell/\sigma)]$ of the resulting facilitated relaxation, where $\nu \sim \mathcal{O}(1)$ is a constant, $\ell(M)$ is the average length scale between fundamental relaxations, and $\sigma(M)$ is their size [23]. By applying this reasoning to ΔH data from BDS [29], we recently suggested that the ratio of α and β barriers at T_g obeys

$$\mathcal{R}(M) \equiv \frac{\Delta H_\alpha(M)}{\Delta H_\beta(M)} = \left[1 + \nu \log\left(\frac{\ell(M)}{\sigma(M)}\right)\right], \qquad (1)$$

which is proportional to the maximum number of β events that act in sync to facilitate the α relaxation [29,79]. This is in the spirit of the suggestion by Fujimori and Oguni [80] that $\mathcal{R}$ varies with the size of the correlation region in glass formers. The simple long-chain relation $\mathcal{R} \simeq \frac{1}{24}\log(100\ \mathrm{s}/\tau_0)$ breaks down at smaller molecular weights ($M < M^{\star\star}$) in stiff polymers, where intramolecular facilitation plays a role in the structural relaxation.

Discussion—The remarkable similarity between the M dependence of the barrier ratio $\mathcal{R}(M)$ and $N_c(M)$ is more difficult to interpret, and even though dynamic facilitation directly implies dynamic heterogeneities [23], DHs can exist without DF [19]. However, the growing evidence for DF in glass-forming systems [22,23,29,81–84] makes it increasingly important to identify links between DF properties, such as $\mathcal{R}(M)$, and the size of DHs, as reflected in $N_c(M)$ or the corresponding characteristic length scale ξ_{DH} [85]. Computer simulations and experiments [22,87–89] have investigated the T-dependent geometry of DHs, with several studies finding that dynamic clusters (CRRs) become increasingly compact near T_g, so that the characteristic length scale $\xi_{\mathrm{DH}} \propto N_c^\gamma$ with $\gamma \approx 1/3$. If we use the simple approximation of compact CRRs, then the corresponding length $\xi_{\mathrm{DH}}(M) \sim N_c(M)^{-1/3}$ roughly scales with $\mathcal{R}(M)$ (Fig. 3; see Fig. S8 of Supplemental Material [43] for more discussion). Following the DF interpretation [29,79], the ratio $\mathcal{R}$ corresponds to the maximum number of β relaxation beads that need to be jointly activated to facilitate the structural α relaxation.

Several recent computational studies have uncovered relations between DF and secondary relaxation contributions. Recent simulations by Guiselin *et al.* [82] and Scalliet *et al.* [83] used a swap Monte Carlo technique to access equilibrated temperatures near T_g, finding that slow regions relax by DF by spreading of mobility from more localized relaxations situated within an "excess wing" on the high-frequency side of the structural α relaxation response (analogous to our picture of β relaxations facilitating the α relaxation). Ortlieb *et al.* [22] combined simulations with experiments on a colloidal glass former [22], finding that each "particle" participating in a CRR takes part in many excitations (DF) during the lifetime ($\sim\tau_\alpha$) of a CRR, leading the authors to speculate that CRRs form by accumulation of excitations [90]. Finally, Nishikawa and Berthier [84] demonstrated that, in a three-dimensional lattice glass model near T_g, structural relaxation is driven by a small population of mobile particles (with low activation barriers) acting as emerging quasiparticles that drive DH.

Conclusion—We demonstrate how chain length and chain flexibility affect dynamic heterogeneities in linear polymers. Highly flexible polymers show simpler behavior with chain-length-independent dynamic heterogeneity, whereas less flexible polymers show a complex chain-length dependence resulting from an interplay between intra- and intermolecular cooperativity. Our results provide a benchmark for new theories and models of glass formation in polymers and other glass formers with internal degrees of freedom coupled to molecular motion.

Acknowledgments—We thank Caroline Crauste for helpful discussions. We acknowledge the Engineering and Physical Sciences Research Council (EPSRC) for financial support (No. EP/M009521/1, No. EP/P505593/1, and No. EP/M506552/1). P. D. O. thanks Georgetown University and the Ives Foundation for support.

Data availability—The data that support the findings of this article are openly available [91].

[1] J. C. Dyre, Colloquium: The glass transition and elastic models of glass-forming liquids, Rev. Mod. Phys. **78**, 953 (2006).

[2] Dynamical arrest into a frozen glassy state occurs at a temperature T_{dyn} near T_g, with a lower T_{dyn} for a slower cooling rate.

[3] H. Sillescu, Heterogeneity at the glass transition: A review, J. Non-Cryst. Solids **243**, 81 (1999).

[4] L. Berthier, G. Biroli, J.-P. Bouchaud, L. Cipeletti, and W. van Saarloos, *Dynamical Heterogeneities in Glasses, Colloids, and Granular Media* (Taylor and Francis, New York, 2011).

[5] E. Donth, The size of cooperatively rearranging regions in polystyrene and styrene-dimethylsiloxane diblock copolymers at the glass transition temperature, Acta Polym. **35**, 120 (1984).

[6] S. Kahle, J. Korus, E. Hempel, R. Unger, S. Höring, K. Schröter, and E. Donth, Glass-transition cooperativity onset in a series of random copolymers poly (n-butyl methacrylate-stat-styrene), Macromolecules **30**, 7214 (1997).

[7] E. Hempel, G. Hempel, A. Hensel, C. Schick, and E. Donth, Characteristic length of dynamic glass transition near T_g for a wide assortment of glass-forming substances, J. Phys. Chem. B **104**, 2460 (2000).

[8] S. Cerveny, J. Mattsson, J. Swenson, and R. Bergman, Relaxations of hydrogen-bonded liquids confined in two-dimensional vermiculite clay, J. Phys. Chem. B **108**, 11596 (2004).

[9] B. Rijal, L. Delbreilh, and A. Saiter, Dynamic heterogeneity and cooperative length scale at dynamic glass transition in glass forming liquids, Macromolecules **48**, 8219 (2015).

[10] U. Tracht, M. Wilhelm, A. Heuer, H. Feng, K. Schmidt-Rohr, and H. W. Spiess, Length scale of dynamic heterogeneities at the glass transition determined by multidimensional nuclear magnetic resonance, Phys. Rev. Lett. **81**, 2727 (1998).

[11] E. Donth, The size of cooperatively rearranging regions at the glass transition, J. Non-Cryst. Solids **53**, 325 (1982).

[12] C. Roland, M. Hensel-Bielowka, M. Paluch, and R. Casalini, Superooled dynamics of glass-forming liquids and polymers under hydrostatic pressure, Rep. Prog. Phys. **687**, 1405 (2005).

[13] N. Ito, K. Duvvuri, D. V. Matyushov, and R. Richert, Solvent response and dielectric relaxation in supercooled butyronitrile, J. Chem. Phys. **125**, 024504 (2006).

[14] N. L. Mandel, T. Rehman, and L. J. Kaufman, Manifestations of static and dynamic heterogeneity in single molecule translational measurements in glassy systems, J. Chem. Phys. **157**, 157 (2022).

[15] L. Hong, V. Novikov, and A. P. Sokolov, Is there a connection between fragility of glass forming systems and dynamic heterogeneity/cooperativity?, J. Non-Cryst. Solids **357**, 351 (2011).

[16] L. Hong, P. Gujrati, V. Novikov, and A. Sokolov, Molecular cooperativity in the dynamics of glass-forming systems: A new insight, J. Chem. Phys. **131**, 194511 (2009).

[17] A. I. Melcuk, R. A. Ramos, H. Gould, W. Klein, and R. D. Mountain, Long-lived structures in fragile glass-forming liquids, Phys. Rev. Lett. **75**, 2522 (1995).

[18] J. Horbach, W. Kob, K. Binder, and C. A. Angell, Finite size effects in simulations of glass dynamics, Phys. Rev. E **54**, R5897 (1996).

[19] L. Berthier and G. Biroli, Theoretical perspective on the glass transition and amorphous materials, Rev. Mod. Phys. **83**, 587 (2011).

[20] G. Jung, G. Biroli, and L. Berthier, Predicting dynamic heterogeneity in glass-forming liquids by physics-informed machine learning, Phys. Rev. Lett. **130**, 238202 (2023).

[21] L. Berthier and D. Reichman, Modern computational studies of the glass transition, Nat. Rev. Phys. **5**, 102 (2023).

[22] L. Ortlieb, T. S. Ingebrigtsen, J. E. Hallett, F. Turci, and C. P. Royall, Probing excitations and cooperatively rearranging regions in deeply supercooled liquids, Nat. Commun. **14**, 2621 (2023).

[23] A. S. Keys, L. O. Hedges, J. P. Garrahan, S. C. Glotzer, and D. Chandler, Excitations are localized and relaxation is hierarchical in glass-forming liquids, Phys. Rev. X **1**, 021013 (2011).

[24] ξ_{DH} has been shown to correlate with the activation volume for structural relaxation [defined through the pressure dependence of $\tau_\alpha(T)$], the volumetric contribution to the dynamic fragility, and the properties of the excess in the vibrational density of states compared with the Debye prediction, i.e., the Boson peak [15,25].

[25] E. Bouthegourd, A. Esposito, D. Lourdin, A. Saiter, and J. Saiter, Size of the cooperative rearranging regions vs. fragility in complex glassy systems: Influence of the structure and the molecular interactions, Physica (Amsterdam) **425B**, 83 (2013).

[26] C. J. Ellison, M. K. Mundra, and J. M. Torkelson, Impacts of polystyrene molecular weight and modification to the repeat unit structure on the glass transition- nanoconfinement effect and the cooperativity length scale, Macromolecules **38**, 1767 (2005).

[27] K. Schröter, S. Reissig, E. Hempel, and M. Beiner, From small molecules to polymers: Relaxation behavior of n-butyl methacrylate based systems, J. Non-Cryst. Solids **353**, 3976 (2007).

[28] J. Cowie, Some general features of Tg-M relations for oligomers and amorphous polymers, Eur. Polym. J. **11**, 297 (1975).

[29] D. L. Baker, M. Reynolds, R. Masurel, P. D. Olmsted, and J. Mattsson, Cooperative intramolecular dynamics control the chain-length-dependent glass transition in polymers, Phys. Rev. X **12**, 021047 (2022).

[30] L. Fetters, D. Lohse, D. Richter, T. Witten, and A. Zirkel, Connection between polymer molecular weight, density, chain dimensions, and melt viscoelastic properties, Macromolecules **27**, 4639 (1994).

[31] L. Berthier, G. Biroli, J.-P. Bouchaud, L. Cipelletti, D. El Masri, D. L'Hôte, F. Ladieu, and M. Pierno, Direct experimental evidence of a growing length scale accompanying the glass transition, Science **310**, 1797 (2005).

[32] C. Dalle-Ferrier, C. Thibierge, C. Alba-Simionesco, L. Berthier, G. Biroli, J.-P. Bouchaud, F. Ladieu, D. L'Hôte, and G. Tarjus, Spatial correlations in the dynamics of glassforming liquids: Experimental determination of their temperature dependence, Phys. Rev. E **76**, 041510 (2007).

[33] Y. Rahmani, K. van der Vaart, B. van Dam, Z. Hu, V. Chikkadi, and P. Schall, Dynamic heterogeneity in hard and soft sphere colloidal glasses, Soft Matter **8**, 4264 (2012).

[34] E. Weeks, J. C. Crocker, and D. A. Weitz, Short- and long-range correlated motion observed in colloidal glasses and liquids, J. Phys. Condens. Matter **19**, 205131 (2007).
[35] P. Zhang, J. J. Maldois, Z. Liu, J. Schroers, and P. M. Voyles, Spatially heterogeneous dynamics in a metallic glass forming liquid imaged by electron correlation microscopy, Nat. Commun. **9**, 1129 (2018).
[36] E. Donth, *The Glass Transition: Relaxation Dynamics in Liquids and Disordered Materials*, Vol. 48 (Springer Science & Business Media, New York, 2013).
[37] G. D. Smith, O. Borodin, and D. Bedrov, Quantum chemistry based force field for simulations of poly (propylene oxide) and its oligomers, J. Phys. Chem. A **102**, 10318 (1998).
[38] A. Agapov and A. P. Sokolov, Size of the dynamic bead in polymers, Macromolecules **43**, 9126 (2010).
[39] P. Sundararajan and P. Flory, Configurational characteristics of poly (methyl methacrylate), J. Am. Chem. Soc. **96**, 5025 (1974).
[40] J. S. Smith, O. Borodin, and G. D. Smith, A quantum chemistry based force field for poly (dimethylsiloxane), J. Phys. Chem. B **108**, 20340 (2004).
[41] Bond stretching and bond bending account for the two DOF "lost" upon polymerization, but these DOF do not participate in molecular motions for polymers with high dihedral barriers and large bending energies.
[42] A. Kudlik, S. Benkhof, T. Blochowicz, C. Tschirwitz, and E. Rössler, The dielectric response of simple organic glass formers, J. Mol. Struct. **479**, 201 (1999).
[43] See Supplemental Material at http://link.aps.org/supplemental/10.1103/p5r4-2g4q for information about the calorimetry, dielectric spectroscopy, and additional data, which includes Refs. [44–67].
[44] S. Weyer, A. Hensel, and C. Schick, Phase angle correction for TMDSC in the glass-transition region, Thermochim. Acta **304**, 267 (1997).
[45] A. Hensel and C. Schick, Relation between freezing-in due to linear cooling and the dynamic glass transition temperature by temperature-modulated DSC, J. Non-Cryst. Solids **235**, 510 (1998).
[46] V. Bershtein and V. Yegorov, General mechanism of the β transition in polymers, Polym. Sci. USSR **27**, 2743 (1985).
[47] V. Bershtein, V. Egorov, L. Egorova, and V. Ryzhov, The role of the thermal analysis in revealing the common molecular nature of transitions in polymers, Thermochim. Acta **238**, 41 (1994).
[48] A. Alegria, O. Mitxelena, and J. Colmenero, On the molecular motions originating from the dielectric γ relaxation of bisphenol-a polycarbonate, Macromolecules **39**, 2691 (2006).
[49] A. Alegria, S. Arrese-Igor, O. Mitxelena, and J. Colmenero, Dielectric secondary relaxation and phenylene ring dynamics in bisphenol-a polycarbonate, J. Non-Cryst. Solids **353**, 4262 (2007).
[50] G. Floudas, J. Higgins, G. Meier, F. Kremer, and E. Fischer, Dynamics of bisphenol-a polycarbonate in the glassy and rubbery state as studied by neutron scattering and complementary techniques, Macromolecules **26**, 1676 (1993).
[51] T. Böhmer, F. Pabst, J.-P. Gabriel, R. Zeissler, and T. Blochowicz, On the spectral shape of the structural relaxation in supercooled liquids, J. Chem. Phys. **162**, 120902 (2025).
[52] A. Kudlik, S. Benkhof, R. Lenk, and E. Rössler, Spectral shape of the α-process in supercooled liquids revisited, Europhys. Lett. **32**, 511 (1995).
[53] R. Leheny, N. Menon, and S. Nagel, Comment on: "spectral shape of the α process in supercooled liquids revisited," Europhys. Lett. **36**, 473 (1996).
[54] R. Leheny, N. Menon, and S. Nagel, Reply to comment on "spectral shape of the α-process in supercooled liquids revisited," Europhys. Lett. **36**, 475 (1996).
[55] R. Bergman, J. Mattsson, C. Svanberg, G. Schwartz, and J. Swenson, Confinement effects on the excess wing in the dielectric loss of glass-formers, Europhys. Lett. **64**, 675 (2003).
[56] C. Svanberg, R. Bergman, and P. Jacobsson, Secondary relaxation in confined and bulk propylene carbonate, Europhys. Lett. **64**, 358 (2003).
[57] T. Blochowicz and E. A. Rössler, Beta relaxation versus high frequency wing in the dielectric spectra of a binary molecular glass former, Phys. Rev. Lett. **92**, 225701 (2004).
[58] J. Mattsson, R. Bergman, P. Jacobsson, and L. Börjesson, Effects of hydrogen bonding on supercooled liquid dynamics and the implication for supercooled water, Phys. Rev. B **79**, 174205 (2009).
[59] C. Gainaru, W. Hiller, and R. Böhmer, A dielectric study of oligo- and poly(propylene glycol), Macromolecules **43**, 1907 (2010).
[60] K. Kaminski, W. Kipnusu, K. Adrjanowicz, E. Mapesa, C. Iacob, M. Jasiurkowska, P. Wlodarczyk, K. Grzybowska, M. Paluch, and F. Kremer, Comparative study on the molecular dynamics of a series of polypropylene glycols, Macromolecules **46**, 1973 (2013).
[61] J. Sjöstrom, R. Bergman, C. Wadell, T. Moberg, and J. Swenson, Effects of water contamination on the supercooled dynamics of a hydrogen-bonded model glass former, J. Phys. Chem. B **115**, 1842 (2011).
[62] J. Mattsson, R. Bergman, P. Jacobsson, and L. Börjesson, Chain-length-dependent relaxation scenarios in an oligomeric glass-forming system: From merged to well-separated α and β loss peaks, Phys. Rev. Lett. **90**, 075702 (2003).
[63] C. Gainaru, W. Hiller, and R. Böhmer, A dielectric study of oligo-and poly (propylene glycol), Macromolecules **43**, 1907 (2010).
[64] K. Kunal, M. Paluch, C. Roland, J. Puskas, Y. Chen, and A. Soklov, Polyisobutylene: A most unusual polymer, J. Polym. Sci.: Part B: Polym. Phys. **46**, 1390 (2008).
[65] K. Ngai, Relation between some secondary relaxations and the α relaxations in glass-forming materials according to the coupling model, J. Chem. Phys. **109**, 6982 (1998).
[66] A. Sokolov, V. Novikov, and Y. Ding, Why many polymers are so fragile, J. Phys. Condens. Matter **19**, 205116 (2007).
[67] C. Dalle-Ferrier, A. Kisliuk, L. Hong, G. Carini, Jr., G. Carini, G. D'Angelo, C. Alba-Simionesco, V. Novikov, and A. Sokolov, Why many polymers are so fragile: A new perspective, J. Chem. Phys. **145**, 154901 (2016).
[68] J. Hintermeyer, A. Herrmann, R. Kahlau, C. Goiceanu, and E. Rossler, Molecular weight dependence of glassy dynamics in linear polymers revisited, Macromolecules **41**, 9335 (2008).
[69] K. Ngai, S. Pawlus, K. Grzybowska, K. Kaminski, S. Capaccioli, and M. Paluch, Does the Johari-Goldstein

β-relaxation exist in polypropylene glycols?, Macromolecules **48**, 4151 (2015).
[70] K. L. Ngai and S. Capaccioli, Relation between the activation energy of the Johari-Goldstein β relaxation and t_g of glass formers, Phys. Rev. E **69**, 031501 (2004).
[71] W. Kauzmann and H. Eyring, The viscous flow of large molecules, J. Am. Chem. Soc. **62**, 3113 (1940).
[72] R. F. Boyer, The relation of transition temperatures to chemical structure in high polymers, Rubber Chem. Technol. **36**, 1303 (1963).
[73] V. A. Bershtein, V. M. Egorov, A. F. Podolsky, and V. A. Stepanov, Interrelationship and common nature of the β relaxation and the glass transition in polymers, J. Polym. Sci., Polym. Lett. Ed. **23**, 371 (1985).
[74] R. H. Boyd, Relaxation processes in crystalline polymers: Molecular interpretation—A review, Polymer **26**, 1123 (1985).
[75] K. Ngai and D. Plazek, Relation of internal rotational isomerism barriers to the flow activation energy of entangled polymer melts in the high-temperature arrhenius region, J. Polym. Sci., Polym. Phys. Ed. **23**, 2159 (1985).
[76] S. Matsuoka and A. Hale, Cooperative relaxation processes in polymers, J. Appl. Polym. Sci. **64**, 77 (1997).
[77] C. M. Roland, S. Hensel-Bielowka, M. Paluch, and R. Caslini, Supercooled dynamics of glass-forming liquids and polymers under hydrostatic pressure, Rep. Prog. Phys. **68**, 1405 (2005).
[78] P. Sollich and M. R. Evans, Glassy time-scale divergence and anomalous coarsening in a kinetically constrained spin chain, Phys. Rev. Lett. **83**, 3238 (1999).
[79] F. Mauch and J. Jäckle, Recursive dynamics in an asymmetrically constrained kinetic ising chain, Physica (Amsterdam) **262A**, 98 (1999).
[80] H. Fujimori and M. Oguni, Correlation index $T_{g,\alpha} - T_{g,\beta}/T_{g,\alpha}$ and activation energy ratio $\delta\varepsilon_{a,\alpha}/\delta\varepsilon_{a,\beta}$ as parameters characterizing the structure of liquid and glass, Solid State Commun. **94**, 157 (1995).
[81] A. S. Keys, J. P. Garrahan, and D. Chandler, Calorimetric glass transition explained by hierarchical dynamic facilitation, Proc. Natl. Acad. Sci. U.S.A. **110**, 4482 (2013).
[82] B. Guiselin, C. Scalliet, and L. Berthier, Microscopic origin of excess wings in relaxation spectra of supercooled liquids, Nat. Phys. **18**, 468 (2022).
[83] C. Scalliet, B. Guiselin, and L. Berthier, Thirty milliseconds in the life of a supercooled liquid, Phys. Rev. X **12**, 041028 (2022).
[84] Y. Nishikawa and L. Berthier, Collective relaxation dynamics in a three-dimensional lattice glass model, Phys. Rev. Lett. **132**, 067101 (2024).
[85] Note that regions of correlated motion are often referred to in the literature as cooperatively rearranging regions, even though different definitions are often used [22,31,86].
[86] E. Donth, The size of cooperatively rearranging regions at the glass transition, J. Non-Cryst. Solids **53**, 325 (1982).
[87] S. Albert, T. Bauer, M. Michl, G. Biroli, J.-P. Bouchaud, A. Loidl, P. Lunkenheimer, R. Tourbot, C. Wiertel-Gasquet, and F. Ladieu, Fifth-order susceptibility unveils growth of thermodynamic amorphous order in glass-formers, Science **352**, 1308 (2016).
[88] E. Flenner, H. Staley, and G. Szamel, Universal features of dynamic heterogeneity in supercooled liquids, Phys. Rev. Lett. **112**, 097801 (2014).
[89] T. Speck, Modeling non-linear dielectric susceptibilities of supercooled molecular liquids, J. Chem. Phys. **155**, 014506 (2021).
[90] Ortlieb *et al.* [22] defined excitations following the approach used by Keys *et al.* [23].
[91] Matthew Reynolds, Daniel L. Baker, Peter D. Olmsted, Johan Mattsson, Data for: "Chain-Length-Dependent Correlated Molecular Motion in Polymers", University of Leeds Data Repository,10.5518/1780 (2025).
[92] U. Schneider, R. Brand, P. Lunkenheimer, and A. Loidl, Excess wing in the dielectric loss of glass formers: A Johari-Goldstein β-relaxation?, Phys. Rev. Lett. **84**, 5560 (2000).
[93] P. K. Dixon, L. Wu, S. R. Nagel, B. D. Williams, and J. P. Carini, Scaling in the relaxation of supercooled liquids, Phys. Rev. Lett. **65**, 1108 (1990).
[94] R. Casalini and C. Roland, Effect of regioisomerism on the local dynamics of polychlorostyrene, Macromolecules **47**, 4087 (2014).
[95] Since $C_p = C_V + TV\lambda^2/\kappa_T$, where λ is the thermal expansion coefficient and κ_T is the isothermal bulk modulus, the approximation $C_V \simeq c_p$ will slightly overestimate the number of the correlated monomers from Eq. (A1). Hempel *et al.* [7] calculated a correction factor based on data for both small molecular and polymeric glass formers, which if applied would increase the determined correlation volume values by $\approx$3%. However, since (i) the correction factor is small, (ii) we do not know how the correction varies for the different chemistries, or M, investigated here, and (iii) a correction will not affect the conclusions of this Letter, we follow the approach normally used in literature and approximate $c_V \approx c_p$.
[96] The amplitude-renormalized $c_p''(T)$ peaks (inset to Fig. 4) show a broadening δT with increasing M. The asymmetry for longer PMMA chains is due to vitrification effects below T_g [45], so the temperature range of the Gaussian fit was limited to $T \gtrsim T_g$. Qualitatively similar trends (T_α and δT increasing with M) are observed for PS and PDMS (see Fig. S3 in [43]). The increase in δT is more prominent in PMMA and PS than in the more flexible PPG-DME and PDMS.
[97] The excess wing has commonly been attributed to a "hidden" β relaxation [12,62,92] or, alternatively, to an intrinsic feature of the α relaxation [93].

End Matter

We use two different methods for estimating the number of dynamically correlated units involved in the α relaxation. In the first approach due to Donth [11], the mean square temperature fluctuations δT^2 within a rearranging region are related to the breadth δT of the calorimetric glass transition response in c_p'' and, in turn, to the volume V_c of the correlated regions by $V_c = k_B T_\alpha^2 \Delta c_V^{-1}/(\rho \delta T^2)$ [3,11].

The peak in $c_p''(T)$ occurs at T_α, ρ is the mass density, and $\Delta c_V^{-1} = c_{V,g}^{-1} - c_{V,l}^{-1}$ is the difference in reciprocal isochoric specific heat of the glassy and liquid states at T_α. The number of monomers $N_c = \rho V_c N_A / M_0$ taking part in correlated motion can be estimated as

$$N_c(M,P) = \frac{k_B N_A T_\alpha^2 \Delta c_V^{-1}}{M_0 \delta T^2}, \tag{A1}$$

where N_A is Avogadro's number, M_0 is the monomer molar mass, and P is the period of the TMDSC oscillation.

TMDSC measurements were performed on PMMA, PS, PPG-DME, and PDMS, as described in Supplemental Material [43], yielding the complex specific heat capacity $c_p^*(T) = c_p'(T) - ic_p''(T)$. The real component $c_p'(T)$ has a step across the glass transition (see Fig. S1 of [43]), which yields Δc_p^{-1}. The imaginary component $c_p''(T)$ shows a peak at the transition temperature T_α; T_α and δT were calculated based on a Gaussian fit to $c_p''(T)$ as in [45]. We follow the literature [7,9,94] and approximate $c_V \approx c_p$, which slightly overestimates N_c but does not affect our conclusions [95].

$c_p''(T;M)$ are shown for PMMA in Fig. 4, measured using a modulation period $P = 60$ s, corresponding to $\tau_\alpha \approx 10$ s. A clear increase in the peak temperatures T_α and in the peak broadening δT [96] are observed with increasing M. As shown in Fig. S5 (Supplemental Material [43]), the variation with molecular weight is smaller for the flexible polymers PPG-DME and PDMS than for PMMA or PS, which is expected due the higher chain flexibility of PPG-DME and PDMS [29] that leads to a smaller variation in T_g.

The second method uses BDS to estimate the number of monomers within a dynamic correlation volume, using the fluctuation-dissipation-based approach of Berthier *et al.* [31,32]. They showed that a "three-point" dynamic susceptibility is a lower bound to χ_4, so that the number of dynamically correlated monomers $N_c^{(4)}(T)$ is

$$N_c^{(4)}(T) \approx \frac{k_B N_A}{m_0 \Delta c_P} T^2 \max_\omega \left\{ \left| \frac{d\chi(\omega,T)}{dT} \right| \right\}^2, \tag{A2}$$

where $m_0 \Delta c_p$ is the difference in isobaric monomer molar heat capacity between the liquid and glass, and $\chi(\omega,T) = [\varepsilon'(\omega,T) - \varepsilon_\infty(T)]/[\varepsilon'(0,T) - \varepsilon_\infty(T)]$ is the normalized dynamic susceptibility [32]. Here, $\varepsilon'(\omega,T)$ is the real component of the complex permittivity and $\varepsilon_\infty(T)$ is its high-frequency limit. The structural relaxation times $\tau_\alpha(T)$ associated with the response $\chi(\omega,T)$ were determined using the fitting approach described in Supplemental Material [43], which allowed conversion from $N_c^{(4)}(T)$ to $N_c^{(4)}(\tau_\alpha)$.

Figure 5 shows $N_c^{(4)}(\tau_\alpha)$ for PMMA and PPG-DME from BDS data (open symbols) compared with N_c calculated for $\tau_\alpha \approx 10$ s from TMDSC data (solid symbols). In both cases, extrapolation of the BDS data shows that $N_c^{(4)}(10\text{ s}) \simeq N_c$. For PMMA, $N_c^{(4)}(\tau_\alpha)$ was only calculated for oligomers ($n = 2-7$), since for longer chains the α relaxation response is increasingly obscured by a strong secondary

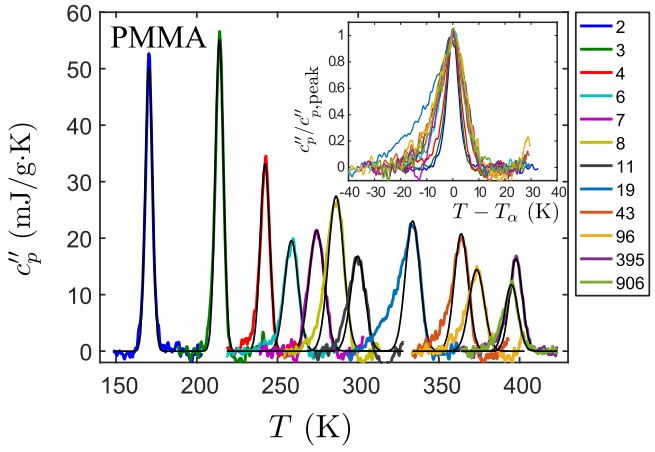

FIG. 4. The imaginary part of the T-dependent specific heat $c_p''(T)$ for PMMA. The legend shows the degree of polymerization n. The peak in $c_p''(T)$ corresponds to the response due to the structural α relaxation, with Gaussian fits (black lines). The inset shows all $c_p''(T)$ data normalized and centered on the peak temperature T_α.

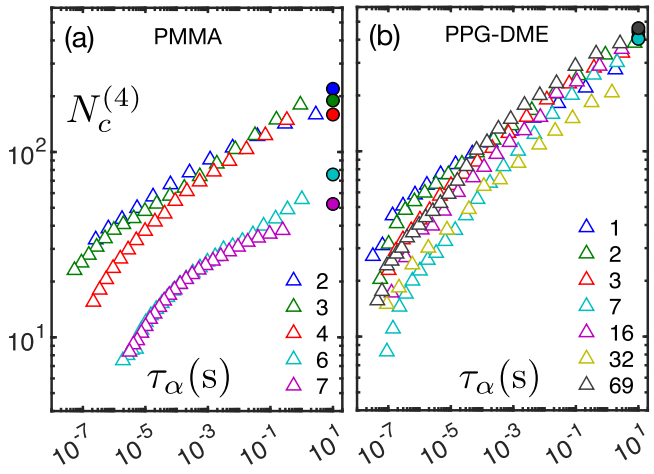

FIG. 5. The number of monomers $N_c^{(4)}$ (△) undergoing correlated motion during the structural α relaxation for (a) PMMA and (b) PPG-DME, determined using BDS, as a function of the α relaxation time τ_α, for n noted in the legends. The extrapolation of $N_c^{(4)}$ to $\tau_\alpha = 10$ s agrees with the corresponding value $N_c(\tau_\alpha = 10\text{ s})$ from TMDSC (●).

β relaxation [29], hindering an accurate determination of $\chi(\omega, T)$. The corresponding plots for PS and PDMS are shown in Fig. S7 of [43]. For PDMS, we generally find good correspondence between $N_c^{(4)}(10\ \mathrm{s})$ and N_c. For PS, a so-called excess wing [68,93] on the high-frequency flank of the α relaxation obscures the α response [97], which increases the uncertainty in the absolute values of $N_c^{(4)}(\tau_\alpha)$. However, $N_c^{(4)}$ increases monotonically with τ_α, and both $N_c^{(4)}$ and N_c show a similar variation with chain length for $\tau_\alpha \sim 10$ s.